Analysis of condition for uniform lighting generated by array of light emitting diodes with large view angle

Zong Qin,[1, 2] Kai Wang,[1,3] Fei Chen,[1,3] Xiaobing Luo[1,4] and Sheng Liu[1,2,3,*]

[1]*Division of MOEMS, Wuhan National Laboratory for Optoelectronics, Wuhan 430074, China*
[2]*Institute for Microsystems, School of Mechanical Science and Engineering, Huazhong University of Science & Technology, Wuhan 430074, China*
[3]*School of Optoelectronics Science and Engineering, Huazhong University of Science & Technology, Wuhan 430074, China*
[4]*School of Energy and Power Engineering, Huazhong University of Science & Technology, Wuhan 430074, China*
**victor_liu63@126.com*

Abstract: In this research, the condition for uniform lighting generated by array of LEDs with large view angle was studied. The luminous intensity distribution of LED is not monotone decreasing with view angle. A LED with freeform lens was designed as an example for analysis. In a system based on LEDs designed in house with a thickness of 20mm and rectangular arrangement, the condition for uniform lighting was derived and the analytical results demonstrated that the uniformity was not decreasing monotonously with the increasing of LED-to-LED spacing. The illuminance uniformities were calculated with Monte Carlo ray tracing simulations and the uniformity was found to increase with the increasing of certain LED-to-LED spacings anomalously. Another type of large view angle LED and different arrangements were discussed in addition. Both analysis and simulation results showed that the method is available for LED array lighting system design on the basis of large view angle LED..

OCIS codes: (230.3670) Light-emitting diodes; (220.2945) Illuminance design; (080.4295) Nonimaging optical systems; (350.4600) Optical engineering.

References and links

1. M. G. Craford, "LEDs for solid state lighting and other emerging applications: status, trends, and challenges," Proc. SPIE, Vol. **5941**, 1–10 (2005).
2. J. Kovác, J. Jakabovic, and M. Kytka, "Advanced light emitting devices for optoelectronic applications," Proc. SPIE **7138**, 71382A (2008).
3. E. F. Schubert, J.-K. Kim, H. Luo, and J.-Q. Xi, "Solid-state lighting—a benevolent technology," Rep. Prog. Phys. **69**(12 Issue 12), 3069–3099 (2006).
4. C.-C. Sun, I. Moreno, S.-H. Chung, W.-T. Chien, C.-T. Hsieh, and T.-H. Yang, "Direct LED backlight for large area LCD TVs: brightness analysis," Proc. SPIE **6669**, 666909 (2007).
5. I. Moreno, and R. I. Tzonchev, "Effects on illuminance uniformity due to dilution on arrays of LEDs," Proc. SPIE **5529**, 268–275 (2004).
6. I. Moreno, M. Avendaño-Alejo, and R. I. Tzonchev, "Designing light-emitting diode arrays for uniform near-field irradiance," Appl. Opt. **45**(10), 2265–2272 (2006), http://www.opticsinfobase.org/ao/abstract.cfm?URI=ao-45-10-2265.
7. I. Moreno, "Configurations of LED arrays for uniform illuminance," Proc. SPIE **5622**, 713–718 (2004).
8. A. J.-W. Whang, Y.-Y. Chen, and Y.-T. Teng, "Designing Uniform Illuminance Systems by Surface-Tailored Lens and Configurations of LED Arrays," J. Disp. Technol. **5**(3), 94–103 (2009), http://www.opticsinfobase.org/jdt/abstract.cfm?URI=jdt-5-3-94.
9. F. Zhao, and J. F. Van Derlofske, "Side-emitting illuminators using LED sources," Proc. SPIE **5186**, 33–43 (2003).
10. W. A. Hendricks, and K. W. Robey, "The sampling distribution of the coefficient of variation," Ann. Math. Stat. **7**(3), 129–132 (1936).
11. H. Yang, J. W. M. Bergmans, T. C. W. Schenk, J.-P. M. G. Linnartz, and R. Rietman, "Uniform illuminance rendering using an array of LEDs: a signal processing perspective," IEEE Trans. Signal Process. **57**(3 Issue 3), 1044–1057 (2009).
12. I. Moreno, and C.-C. Sun, "LED array: Where does far-field begin?" Proc. SPIE **7058**, 70580R (2008).

#128952 - $15.00 USD Received 24 May 2010; revised 26 Jun 2010; accepted 12 Jul 2010; published 30 Jul 2010

13. I. Moreno, C.-C. Sun, and R. Ivanov, "Far-field condition for light-emitting diode arrays," Appl. Opt. **48**(6), 1190–1197 (2009), http://www.opticsinfobase.org/ao/abstract.cfm?URI=ao-48-6-1190.
14. R. Barakat, "Application of Apodization to Increase Two-Point Resolution by the Sparrow Criterion. I. Coherent Illuminance," J. Opt. Soc. Am. **52**(3), 276–279 (1962), http://www.opticsinfobase.org/josa/abstract.cfm?URI=josa-52-3-276.
15. J. L. Harris, "Diffraction and Resolving Power," J. Opt. Soc. Am. **54**(7), 931–933 (1964), http://www.opticsinfobase.org/josa/abstract.cfm?URI=josa-54-7-931.
16. C. Sparrow, "On spectroscopic resolving power," Astrophys. J. **44**, 76 (1916).
17. K. Wang, F. Chen, Z. Y. Liu, X. B. Luo, and S. Liu, "Design of compact freeform lens for application specific Light-Emitting Diode packaging," Opt. Express **18**(2), 413–425 (2010), http://www.opticsinfobase.org/abstract.cfm?URI=oe-18-2-413.
18. F. Chen, S. Liu, K. Wang, Z. Y. Liu, and X. B. Luo, "Free-form lenses for high illuminance quality light-emitting diode MR16 lamps," Opt. Eng. **48**(12), 123002 (2009).
19. I. Moreno, and C.-C. Sun, "Modeling the radiation pattern of LEDs," Opt. Express **16**(3), 1808–1819 (2008), http://www.opticsinfobase.org/oe/abstract.cfm?URI=oe-16-3-1808.
20. I. Moreno, C.-Y. Tsai, D. Bermúdez, and C.-C. Sun, "Simple function for luminous intensity distribution from LEDs," Proc. SPIE **6670**, 66700H (2007).

1. Introduction

Nowadays, LED technology has been so widely used that traditional sources are being replaced by LEDs quickly in applications such as automobile lighting, roadway lighting, indoor lighting, backlighting, etc., due to LEDs' irresistible advantages of low energy consumption, long life time, pollution-free materials, varieties of color options and so on [1–3]. A critical technology in LED lighting is how to achieve a plane with uniform illuminance distribution, which is generated by a LED system as thin as possible. For instance, a LED backlighting module is always decided to provide uniform illuminance on LCD panel and meanwhile meets the thickness requirement of flat panel display [4].

A common solution of uniform illuminance is to place a planar array of LEDs under the target plane, which is called LED array lighting (LAL), to acquire the desired illuminance distribution wherein the illuminance uniformity is decided by configuration of the LED array and the distance from LEDs to the target plane. In general, better illuminance uniformity could be obtained by smaller LED-to-LED spacing and larger distance from LEDs to the target plane [5].

Computer simulation is useful to verify this kind of problem by simulating every possible solution. However, it is a better choice to solve it with a quantitative method in order to save simulation time. Simulations cannot even lead to an optimum solution sometimes. Moreno Ivan etc. advanced the design method of LAL system based on generalized Lambertian LED [5–8], which can figure out some key parameters of acquiring a uniform illuminance distribution generated by LED array of different configurations and distances from the array to the target plane.

The package density of LED array in a LAL system can be reduced by enlarging the view angle of LED with a constant thickness and vice versa [9]. But it is hard to describe the luminous intensity distribution of a large view angle LED with the generalized Lambertian function. In this study, a LED with freeform lens that can produce a circular light pattern is designed as an example of large view angle LED. The condition for uniform lighting generated by a rectangular array based on this type of LED was derived and the illuminance uniformities were calculated.

Illuminance uniformity is an important concept in this paper, which is defined as CV(RMSE), as the abbreviation of coefficient of variation of root mean square error [10, 11]. A group of pints on the observation plane are sampled and the value of CV(RMSE) is the ratio of the RMSE (same as the standard error here) to the mean value of the samples, as shown in Eq. (1). A smaller value represents a higher uniformity. This definition of uniformity is conventional in image processing. The reciprocal ratio of CV(RMSE) is known as the signal to noise ratio of the image.

$$CV(RMSE) = RMSE / \bar{x} \ \ or \ \ \sigma / \bar{x} \tag{1}$$

#128952 - $15.00 USD Received 24 May 2010; revised 26 Jun 2010; accepted 12 Jul 2010; published 30 Jul 2010

where $\bar{x}$ is the mean value and σ is the standard error of the samples.

The condition for uniform illuminance distribution was derived and several separations that may lead to uniform lighting were found. The derivation was verified by simulating. Both the theoretical analysis and simulation results demonstrated that the illuminance uniformity of the target plane is not monotone decreasing with the increasing of the separation between LEDs. For example, in a LAL system with a thickness of 20mm, rectangular array arrangement and LEDs designed in house, CV(RMSE) of the observation plane decreases from 0.261 to 0.148 when the LED-to-LED spacing increases from 72.33mm to 83.78mm.Similar non-decreasing happens to other two pairs of separations.

Another type of large view angle LED and different arrangements of LED array were discussed in addition.

LAL system based on large view angle LED exhibits quite different properties from that based on generalized Lambertian LED. Referring to the method proposed in this paper, it is convenient and time-saving for designers to select the optimum configuration of LED array by combining the specific demands of applications. And the non-monotone-decreasing must be noted.

2. Introduction to the LAL design method based on generalized Lambertian LED

Considering that a planar region with uniform illuminance is generated by a rectangular 2 × 2 LED array, all the LEDs can be assumed to be point sources [12, 13] with the same luminous intensity distribution and luminous flux. Meanwhile, the LED-to-LED spacing is d. The target plane is parallel to the LED array with a distance z.

The luminous intensity distribution of generalized Lambertian LED can be expressed in power function of cosine of the view angle, which is given by Eq. (2)

$$I(\theta) = I_0 \cos^m \theta \tag{2}$$

where θ is the view angle of LED. For an ideal Lambertian emitter, m equals to 1. But the light energy distribution will be always slightly different from that of an ideal Lambertian emitter because of the encapsulant and lens of LED packaging, which leads to an m larger or less than 1.

And then, the illuminance E (lm/m^2) of a point on the target plane generated by such a LED at distance r is given by Eq. (3)

$$E(r,\theta) = I(\theta)\cos\theta / r^2 \tag{3}$$

The illuminance E of a point (x,y) on the target plane is generated by a 2 × 2 LED array with LED-to-LED spacing d and vertical distance from the target plane to the array z, as shown in Fig. 1. The expression of illuminance E is given by Eq. (4)

#128952 - $15.00 USD Received 24 May 2010; revised 26 Jun 2010; accepted 12 Jul 2010; published 30 Jul 2010

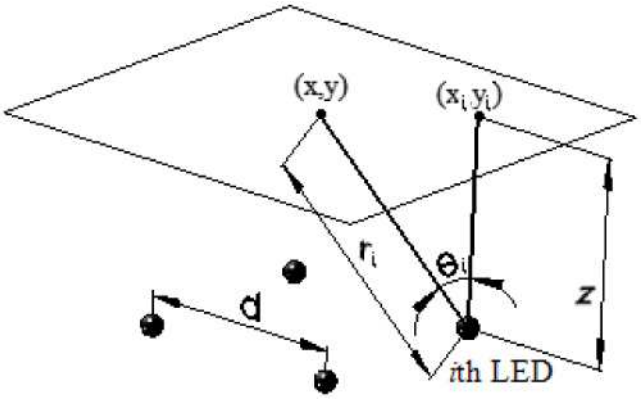

Fig. 1. The illuminance of the point (x,y) is generated by 4 LEDs in 2 × 2 array. Point (0,0) corresponds to the central point of the region enclosed by the 4 LEDs. Parameters to calculate the illuminance generated by the *i*th (i = 1~4) LED are indicated in the figure.

$$E(r,\theta) = \sum_{i=1}^{4} E_i(r_i,\theta_i) \tag{4}$$

By substituting Eq. (2) and Eq. (3) in Eq. (4) and converting to the Cartesian coordinates, $E(x,y)$ is acquired, as given by Eq. (5).

$$E(x,y) = I_0 z^{m+1}\{[(x-\frac{d}{2})^2+(y-\frac{d}{2})^2+z^2]^{-\frac{m+3}{2}} + [(x-\frac{d}{2})^2+(y+\frac{d}{2})^2+z^2]^{-\frac{m+3}{2}} + [(x+\frac{d}{2})^2+(y-\frac{d}{2})^2+z^2]^{-\frac{m+3}{2}} + [(x+\frac{d}{2})^2+(y+\frac{d}{2})^2+z^2]^{-\frac{m+3}{2}}\} \tag{5}$$

Sparrow's Criterion [14–16] was originally used in image resolution to estimate the maximal separation between image points. We can use it to estimate the maximal separation between LEDs. According to Sparrow's Criterion, differentiating $E(x,y)$ twice and setting $\partial^2 E / \partial x^2 = 0$ at x = 0 and y = 0 leads to the maximal LED-to-LED spacing d, as given in Eq. (6), which can guarantee that the illuminance in the region across the central point is invariable.

$$d = \sqrt{\frac{4}{m+3}} \cdot z \tag{6}$$

If z is determined, the maximal suitable LED-to-LED spacing d_m for uniform lighting can be calculated by Eq. (6).

It must be noted that m here is defined according to the luminous intensity while m in references [5–8] is defined according to the illuminance on the target plane, as $E = E_O \cos^m \theta$. As a result of Eq. (3), the two results are slightly different. The difference in value between the two parameters is 1

More LEDs can be considered in the calculation, such as a 4 × 4 or 6 × 6 array, to achieve the condition for uniform lighting for an actual LAL system.

3. Design of a LED lens with large view angle

Since the light emitting from generalized Lambertian LED concentrates in the direction of light axis, larger view angle LEDs are needed if we aim at decreasing the package density of LED array [9]. In general, large view angle LED can be acquired with freeform lens.

Utilizing freeform optics design method [17,18], a freeform LED lens was designed, which can produce a circular light pattern with radius of 60mm on a plane 20mm away, as

#128952 - $15.00 USD Received 24 May 2010; revised 26 Jun 2010; accepted 12 Jul 2010; published 30 Jul 2010

shown in Fig. 2. Using a LED chip with a luminous flux of 1 lumen, the illuminance distribution on a plane 20mm away is simulated by Monte Carlo ray tracing method, as shown in Fig. 3. The luminous intensity distribution curve attached to this type of LED, as shown in Fig. 4, is quite different from that of generalized Lambertian LED that the value of luminous intensity is not monotone decreasing with the increasing of view angle,. We call it a non-monotone-decreasing distribution (NMDD).

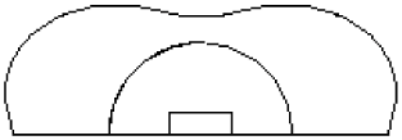

Fig. 2. Freeform lens that can produce a circular light pattern with a radius of 60mm at a plane 20mm away

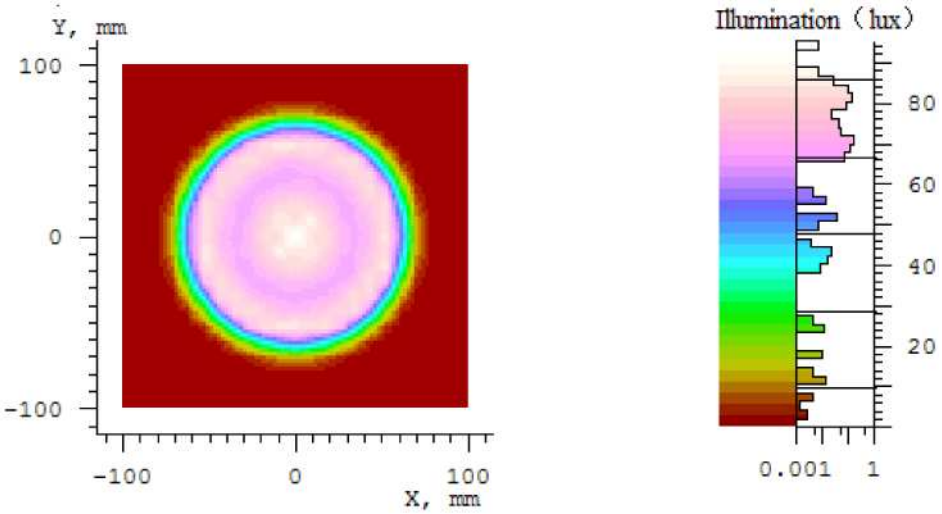

Fig. 3. Simulated illuminance distribution produced by the freeform lens in Fig. 2. Different color in the left sub-figure represents different illuminance value. The relationship between color and illuminance value is shown in the right sub-figure. The right sub-figure also shows how much luminous flux accumulates at each illuminance value.

#128952 - $15.00 USD Received 24 May 2010; revised 26 Jun 2010; accepted 12 Jul 2010; published 30 Jul 2010

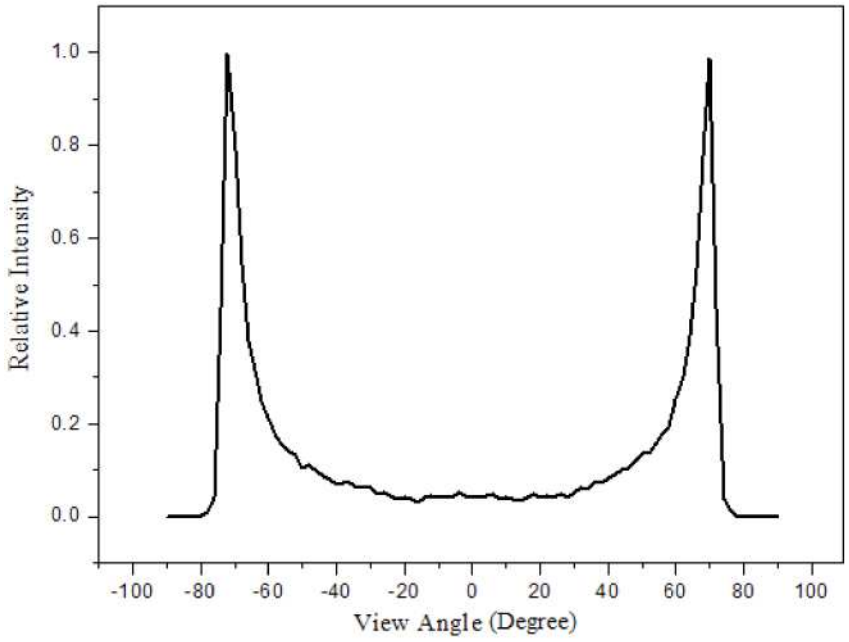

Fig. 4. Luminous intensity distribution curve attached to the circular light pattern in Fig. 3

Obviously, the luminous intensity distribution curve shown in Fig. 4 cannot be fitted with power function of cosine of the view angle as generalized Lambertian LED. However, an analytical curve fitting must be presented to analyze the condition for uniform lighting generated by this type of LED.

The luminous intensity distribution of LED can be usually expressed as sum of power functions of cosine of the view angle or Gaussian functions [19, 20], as given by Eq. (7) and Eq. (8).

$$I(\theta) = \sum_i c1_i \cos(|\theta| - c2_i)^{c3_i} \tag{7}$$

$$I(\theta) = \sum_i g1_i \exp[-(\ln 2)(\frac{|\theta| - g2_i}{g3_i})^2] \tag{8}$$

where, $c1_i$, $c2_i$, $c3_i$, $g1_i$, $g2_i$, $g3_i$ are all parameters to be determined.

Luminous intensity distribution of LED whose energy mostly concentrates in the direction of light axis can be fitted with Eq. (7) while that of large view angle LED can be fitted with Eq. (8). Particularly, Eq. (2) is a simplified form of Eq. (7) and Eq. (8) is needed to fit the distribution curve shown in Fig. (3) and then the quantitative analysis of the condition for uniform lighting can be presented based on the fitting result.

Giving consideration to both accuracy of curve fitting and simplicity of calculation, a three order Gaussian function is utilized where there are 9 parameters to be determined, as given by Eq. (9).

$$I(\theta) = P_1 \exp[-(\ln 2)(\frac{|\theta| - P_2}{P_3})^2] + P_4 \exp[-(\ln 2)(\frac{|\theta| - P_5}{P_6})^2] + P_7 \exp[-(\ln 2)(\frac{|\theta| - P_8}{P_9})^2] \tag{9}$$

The result of iterative fitting with computer is shown in Fig. 5, according to which original distribution curve can be replaced by the fitted one in the following work.

#128952 - $15.00 USD Received 24 May 2010; revised 26 Jun 2010; accepted 12 Jul 2010; published 30 Jul 2010

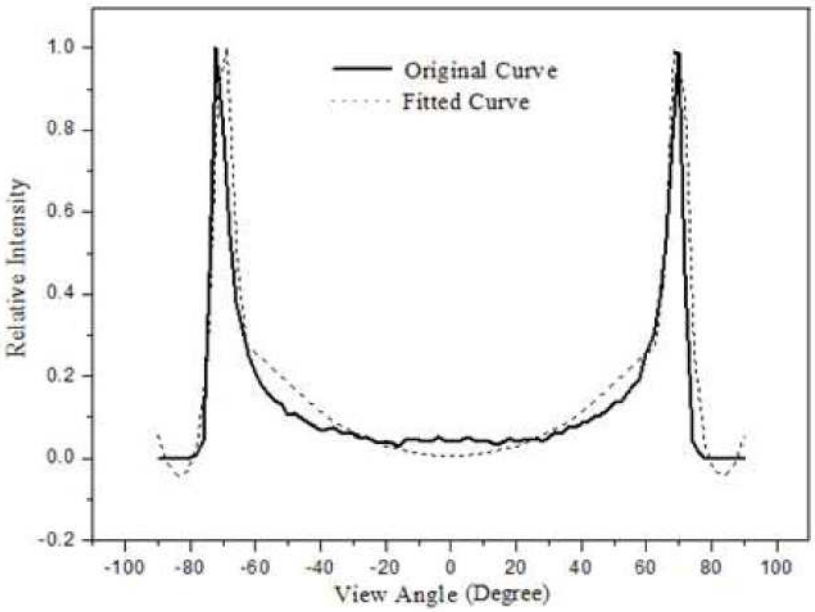

Fig. 5. Fitting result of the NMDD produced by freeform lens where $P_1 = 0.7221$, $P_2 = 1.2212$, $P_3 = 0.0527$, $P_4 = -0.3454$, $P_5 = 1.4540$, $P_6 = 0.1791$, $P_7 = 0.3086$, $P_8 = 1.4767$, $P_9 = 0.5920$ for Eq. (8). Parameters are all in radians although this figure is drawn in degrees

4. Analysis of the condition for uniform lighting generated by NMDD LED array

Similar to the method of analyzing LAL system based on generalized Lambertian LED, the expression of illuminance is derived to advance the condition for uniform lighting generated by NMDD LED array with a rectangular arrangement. The height of target plane z is set to 20mm as the freeform lens is designed for such a height. The LED with freeform lens can be considered as a point source with angular distribution of luminous intensity [12, 13].

In theory, the illuminance of a point is a superposition of the illuminance generated by all LEDs. However, each NMDD LED only generates a 60mm-radius circular light pattern on the target plane. So the illuminance of the gray region in Fig. 6, which is called a "mesh", is only generated by a 4 × 4 array when the separation d>30mm. Moreover, the central point is only illuminated by a 4 × 4 array when d>23.5mm. If d_m got by the calculation is greater than 30mm, the simplification is accurate. The result is still practicable when d_m is less than 30mm slightly.

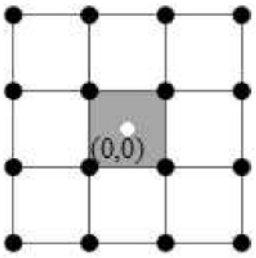

Fig. 6. Model of a LAL system with a 4 × 4 LED array where the illuminance distribution in the gray region will be derived. Black dots states the positions of LEDs. A white dot indicates the origin

#128952 - $15.00 USD Received 24 May 2010; revised 26 Jun 2010; accepted 12 Jul 2010; published 30 Jul 2010

Considering that d_m is about 20mm for a LAL system with z = 20mm and ideal Lambertian LEDs according to Eq. (5), d_m corresponding to such large view angle LEDs is predicted to be greater than 30mm.

E of point (x,y) on the target plane generated by a 4 × 4 LED array is given by Eq. (10)

$$E(r,\theta)=\sum_{i=1}^{16}E_i(r_i,\theta_i)=\sum_{i=1}^{16}\frac{I(\theta_i)\cos\theta_i}{r_i^2} \tag{10}$$

where $I(\theta_i)$ is given by Eq. (8) and the parameters P_1-P_9 are given in Fig. 4.

By converting $E(r,\theta)$ into Cartesian coordinates, $E(x,y)$ is given by Eq. (11)

$$E(x,y)=\sum_{i=1}^{16}E[\sqrt{(x-x_i)^2+(y-y_i)^2+z^2},\arctan(\frac{\sqrt{(x-x_i)^2+(y-y_i)^2}}{z})] \tag{11}$$

where (x_i, y_i) is the position of each LED in the 4 × 4 array.

As each term in Eq. (10) includes a three order Gaussian function, the expanded expression of Eq. (10) will be so complicated that no analytical solution can be obtained by differentiating E(x, y) twice and setting $\partial^2 E/\partial x^2=0$ at x = 0 and y = 0. But Sparrow's Criterion is still available to analyze the condition for uniform lighting.

By differentiating $E(x,y)$ twice and setting x = 0, y = 0 and z = 20mm, a function $f(d)=\partial^2 E/\partial x^2\,|_{x=0,\,y=0,\,z=20}$ is acquired with an independent variable d. According to Sparrow's Criterion [12–14], $f(d)=0$ will lead to an invariable illuminance in the region across the central point. The functional image of $f(d)$ is shown in Fig. 7.

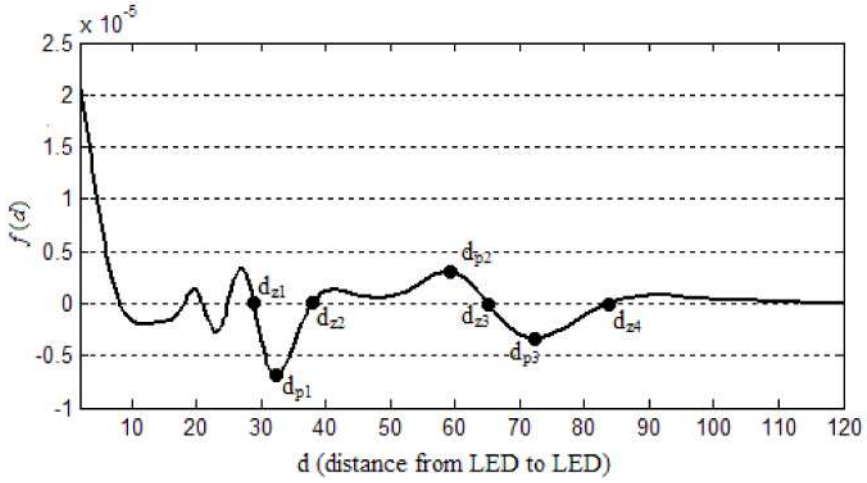

Fig. 7. The functional image of $f(d)=\partial^2 E/\partial x^2\,|_{x=0,\,y=0,\,z=20}$

Differing from the situation of generalized Lambertian LED, there are multiple zero points of $f(d)$ in Fig. 7. Those less than 30mm are not accurate for the actual model due to the simplification. In addition, illuminance distributions corresponding to such small separations are all uniform, which leads the uniformity analysis to lack of sense. So the zero points close to or greater than 30mm, as d_{z1} = 28.90mm, d_{z2} = 37.90mm, d_{z3} = 65.12mm and d_{z4} = 83.78mm, are selected for uniformity analysis. Three peak points, as d_{p1} = 32.44mm, d_{p2} =

#128952 - $15.00 USD Received 24 May 2010; revised 26 Jun 2010; accepted 12 Jul 2010; published 30 Jul 2010

59.11mm and d_{p3} = 72.33mm between every two adjacent zero points are also selected to analyze the monotonicity between uniformity and separations. All selected zero and peak points are marked in Fig. 7.

The one-dimension illuminance distributions in the direction of x axis of the gray region in Fig. 6 corresponding to four zero points are shown in Fig. 8. The values of illuminance are normalized for indicating the variation of illuminance distribution clearly. In theory, the illuminance distribution is same from mesh to mesh. Hence, a finite distribution in Fig. 8 can state the distribution in the whole area. The one-dimension distribution can reflect the two-dimension distribution well due to the rotational symmetry of the luminous intensity distribution of LED.

The illuminance distributions in Fig. 8(a) and Fig. 8(b) can achieve quite a uniform lighting and those in Fig. 8(c) and Fig. 8(d) are less uniform. However, they all can guarantee that the illuminance is invariable in a finite region across the central point. This is because that Sparrow's Criterion decides whether the illuminance is uniform by judging the slope variation of the illuminance across the central point. Some significant variations in the edge region may occur even though Sparrow's Criterion takes effects in the central region. Judged by Sparrow's Criterion, all the four distributions are considered to be "uniform", but in practice, the last two distributions can only satisfy some applications with lower requirements.

The one-dimension illuminance distributions in the direction of x axis of the gray region in Fig. 6 corresponding to three peak points are shown in Fig. 9.

In Fig. 9, slope variations of the illuminance across the central points are not equal to zero in comparison with Fig. 8. These distributions are considered to be nonuniform according to Sparrow's Criterion, although the overall variation may be small enough for some uniformity requirements in spite of the nonzero value of slope variation across the central point. This may happen when the separation is small, such as the distribution in Fig. 9(a).

Comparing the illuminance distribution in Fig. 8(d) with that in Fig. 9(c), the uniformity in Fig. 8(d) is higher, though the separation d_{z4} corresponding to Fig. 8(d) is larger. Referring to the study on LAL system based on generalized Lambertian LED, smaller LED-to-LED spacing leads to a more uniform illuminance distribution if a constant size plane is illuminated by a LED array large enough that the effects of edge LEDs can be ignored [5–8]. But this law is not established to NMDD LED, i.e., the uniformity is not monotone decreasing with the separation between LEDs.

Similar exceptions happen to Fig. 8(c) versus Fig. 9(b) and Fig. 8(b) versus Fig. 9(a). Non-decreasing is found at several pairs of adjacent zero and peak points.

However, the actual 2-dimension illuminance distribution and the monotonicity of uniformity must be verified by simulations or experiments, as operated later.

#128952 - $15.00 USD Received 24 May 2010; revised 26 Jun 2010; accepted 12 Jul 2010; published 30 Jul 2010

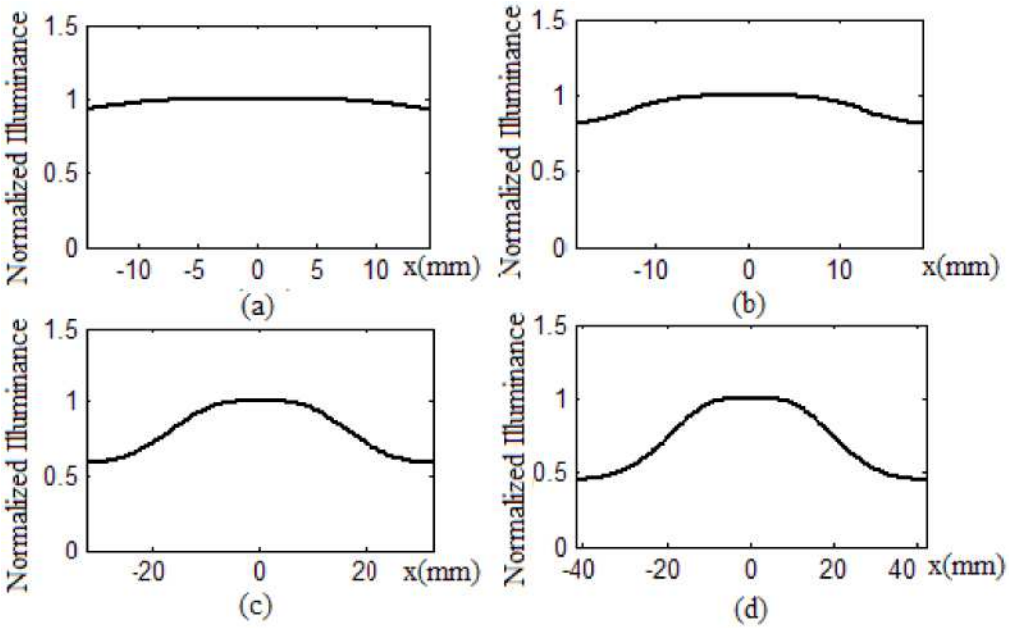

Fig. 8. Illuminance distributions in the direction of x axis of the gray region in Fig. 6 where (a) d_{z1} = 28.90mm, (b) d_{z2} = 37.90mm, (c) d_{z3} = 65.12mm, (d) d_{z4} = 83.78mm

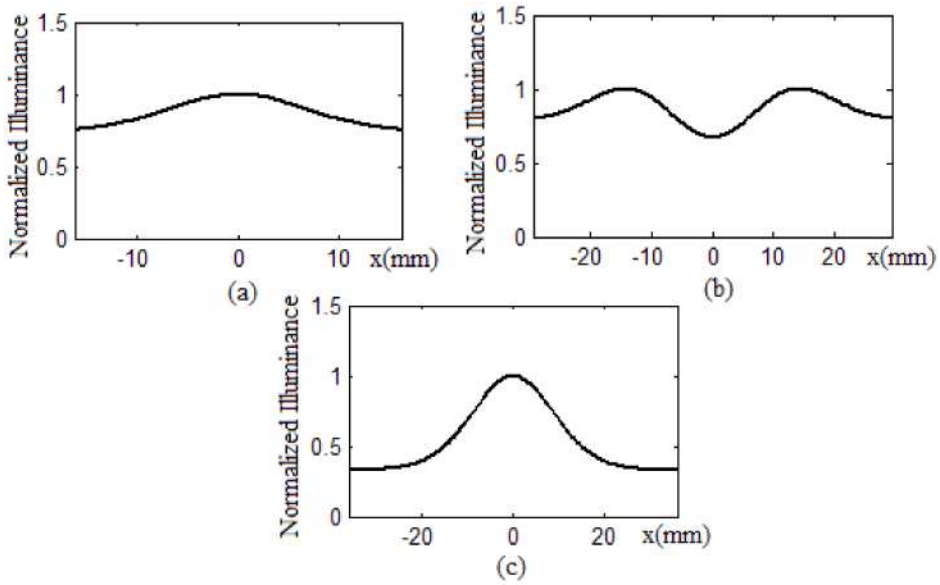

Fig. 9. Illuminance distributions in the direction of x axis of the gray region in Fig. 6 where (a) d_{p1} = 32.44mm, (b) d_{p2} = 59.11mm, (c) d_{p3} = 72.33mm

To verify whether the derivation of illuminance distribution and the analysis of nonmonotonicity are correct, a Monte-Carlo ray tracing simulation approach is utilized to simulate the illuminance distributions on the target plane 20mm away from the LED array.

All the LEDs in simulation are actual models with freeform lens, as the one shown in Fig. 2 and Fig. 3. Large numbers of LED models (more than 100) make up an infinite LED array proximately. A 300mm × 300mm observation plane is constructed 20mm above the

#128952 - $15.00 USD Received 24 May 2010; revised 26 Jun 2010; accepted 12 Jul 2010; published 30 Jul 2010

LED array, which can guarantee that the observation plane corresponds to a 4 × 4 LED array at least. 900 points on the observation plane are sampled to calculate CV(RMSE).

The separation between LEDs is adjusted to d_{z1}, d_{z2}, d_{z3}, d_{z4}, d_{p1}, d_{p2} and d_{p3}.The simulated illuminance distributions on the observation plane are shown in Fig. 10 and Fig. 11. The positions of LED are also stated in these two figures.

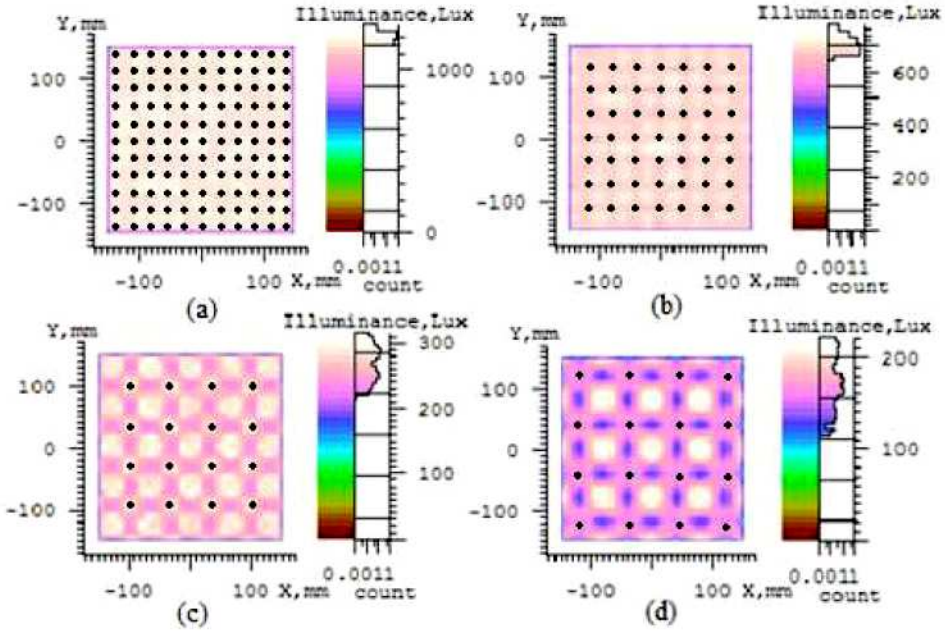

Fig. 10. Simulated illuminance distributions corresponding to zero points (a) d_{z1} = 28.90mm, CV(RMSE) = 0.014 (b) d_{z2} = 37.90mm, CV(RMSE) = 0.032 (c) d_{z3} = 65.12mm, CV(RMSE) = 0.080 (d) d_{z4} = 83.78mm, CV(RMSE) = 0.147. Black dots are used to state positions of LEDs.

In Fig. 10, the illuminance distribution corresponding to zero point d_{z1} is the most uniform with a CV(RMSE) value of 0.014. The CV(RMSE) values corresponding to zero points d_{z2}, d_{z3} and d_{z4} increase to 0.032, 0.080 and 0.147 respectively, which can still meet the requirements of some of applications. What is noteworthy is that the central regions of the area enclosed by 4 LEDs corresponding to d_{z2}, d_{z3} and d_{z4} all assume a bright spot, which is in accordance with the derived result in Fig. 8.

#128952 - $15.00 USD Received 24 May 2010; revised 26 Jun 2010; accepted 12 Jul 2010; published 30 Jul 2010

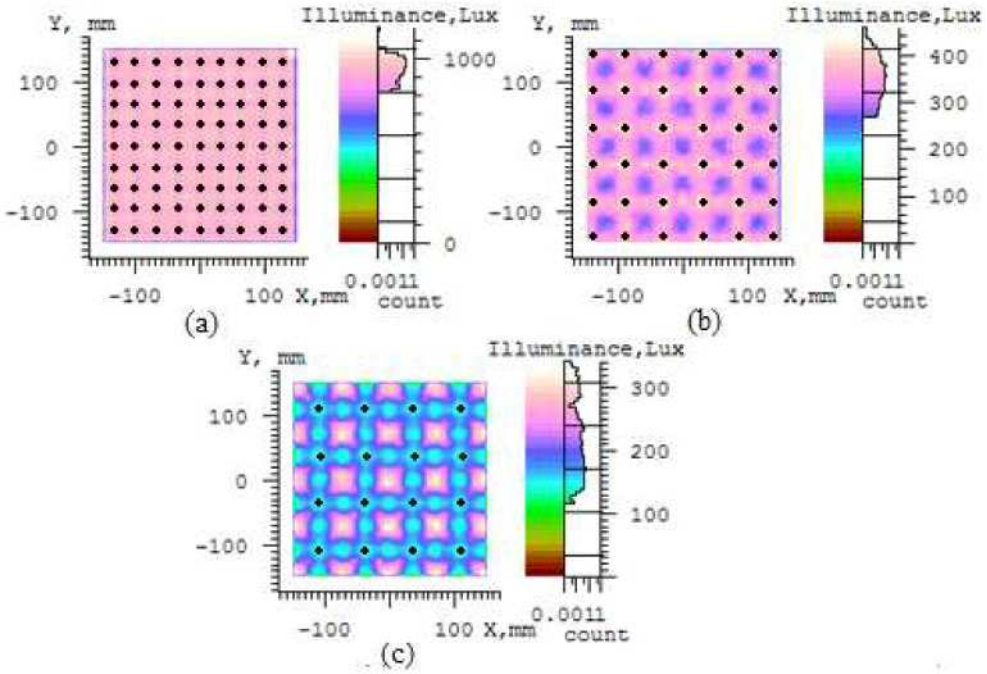

Fig. 11. Simulated illuminance distributions corresponding to peak points (a) d_{p1} = 32.44mm, CV(RMSE) = 0.052 (b) d_{p2} = 59.11mm, CV(RMSE) = 0.107 (c) d_{p3} = 72.33mm, CV(RMSE) = 0.256. Black dots are used to state positions of LEDs.

The illuminance distribution corresponding to d_{p1} in Fig. 11(a) looks quite "uniform" with a CV(RMSE) value of 0.052, which confirms the analysis for Fig. 9 before. The distributions corresponding to d_{p2} and d_{p3} become less uniform. The CV(RMSE) values are 0.107 and 0.256 respectively. Bright spot, dark spot and bright spot are observed sequentially in the central regions of the area enclosed by 4 LEDs in Fig. 11(a), Fig. 11(b) and Fig. 11(c), which is also in accordance with the derived result in Fig. 9.

It must be noted that $d_{p3}<d_{z4}$, but the CV(RMSE) value corresponding to d_{p3} is larger than that corresponding to d_{z4} i.e. the uniformity increases as the separation increases. The non-decreasing happens to d_{p2} versus d_{z3} and d_{p1} versus d_{z2}, which verifies the theoretical analysis of nonmonotonicity based on the derived illuminance distribution in Fig. 8 and Fig. 9.

LUXEON® Batwing LED from Lumileds Philips is another type of large view angle LED. The luminous intensity distribution curve is shown in Fig. 12 that can be fitted by Eq. (12) where P_1 = 0.386, P_2 = 0.08, P_3 = 0369, P_4 = 0.55, P_5 = 0.671and P_6 = 0.153. All the parameters are in radians [19]. A LUXEON® Batwing LED can generate a light pattern with a radius about 20mm on a plane 20mm height, as shown in Fig. 13. Analogously, the illuminance distribution on a target plane 20mm away can be calculated with a 4 × 4 array accurately enough.

#128952 - $15.00 USD Received 24 May 2010; revised 26 Jun 2010; accepted 12 Jul 2010; published 30 Jul 2010

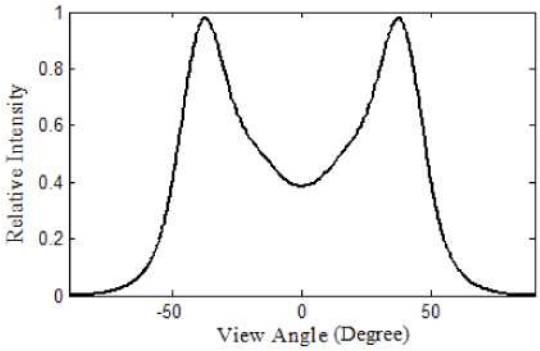

Fig. 12. Luminous intensity distribution curve of LUXEON® Batwing LED from Philips Corporation

$$I(\theta) = P_1 \exp[-(\ln 2)\cdot(\frac{\theta}{P_3})^2]\cos h(P_2 \cdot \frac{180\theta}{\pi}) + P_4 \exp[-(\ln 2)(\frac{|\theta| - P_5}{P_6})^2] \quad (12)$$

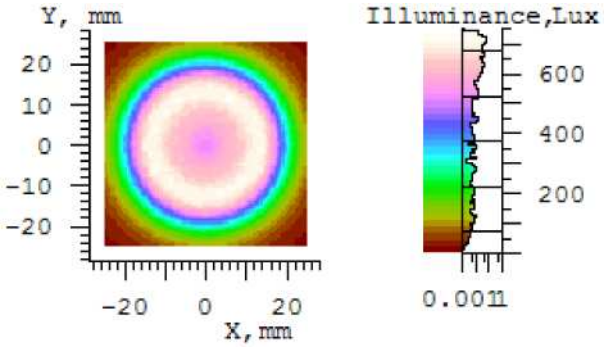

Fig. 13. Simulated illuminance distribution on a 20mm-height plane generated by a LUXEON® Batwing LED from Philips Corporation

Utilizing the method proposed before, the functional image of $f(d)$ is drawn in Fig. 14 by differentiating $E(x, y)$ twice and setting x = 0, y = 0 and z = 20mm□

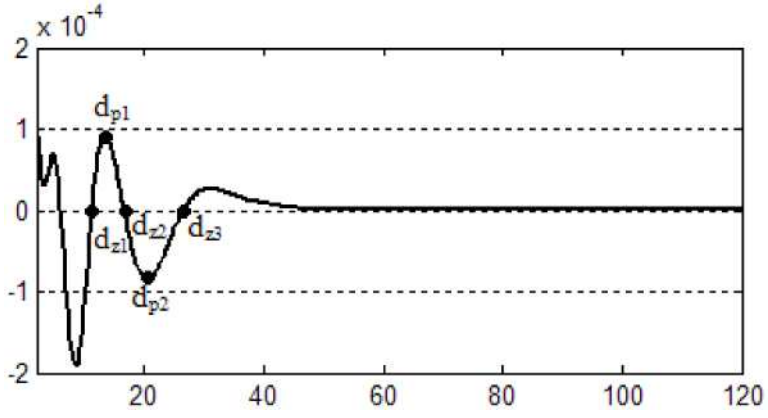

Fig. 14. The functional image of $f(d) = \partial^2 E / \partial x^2 |_{x=0, y=0, z=20}$ for a LUXEON® Batwing LED array

#128952 - $15.00 USD Received 24 May 2010; revised 26 Jun 2010; accepted 12 Jul 2010; published 30 Jul 2010

Three zero points d_{z1} = 11.29mm, d_{z2} = 16.66mm, d_{z3} = 26.56mm and two peak points d_{p1} = 13.41mm, d_{p2} = 20.66mm marked in Fig. 14 are selected for analysis.

The LED model for simulation is provided by Lumileds Philips publicly. A 100mm × 100mm observation plane is constructed and 400 points on it are sampled to calculate CV(RMSE). The simulated illuminance distributions and uniformities are shown in Fig. 15 and Fig. 16.

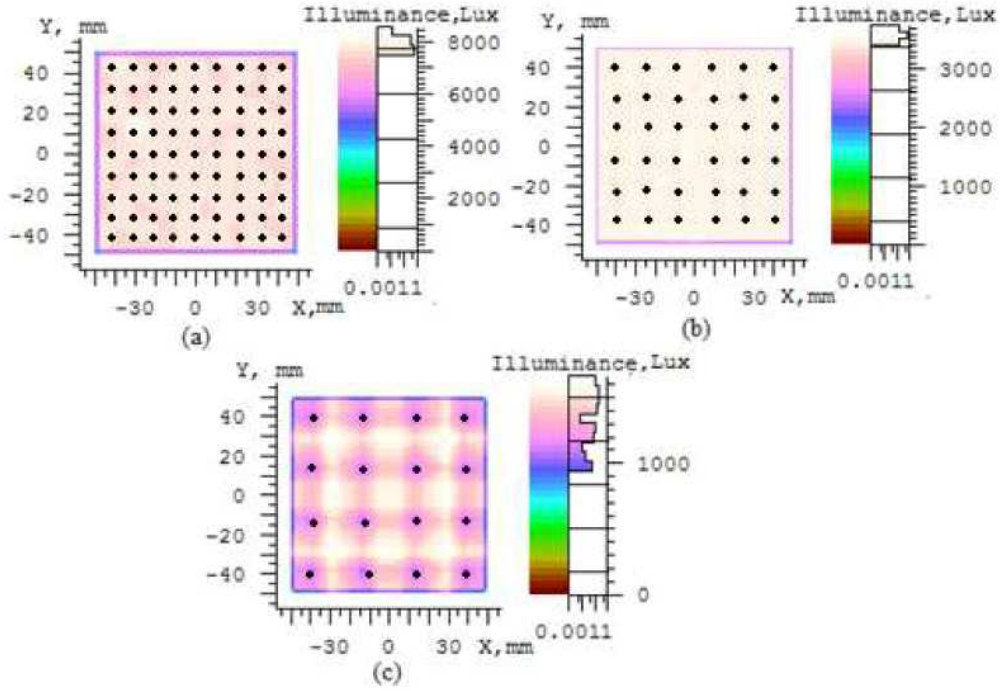

Fig. 15. Simulated illuminance distributions corresponding to zero points (a) d_{z1} = 11.29mm, CV(RMSE) = 0.012 (b) d_{z2} = 16.66mm, CV(RMSE) = 0.016 (c) d_{z3} = 20.66mm, CV(RMSE) = 0.139. Black dots are used to state positions of LEDs.

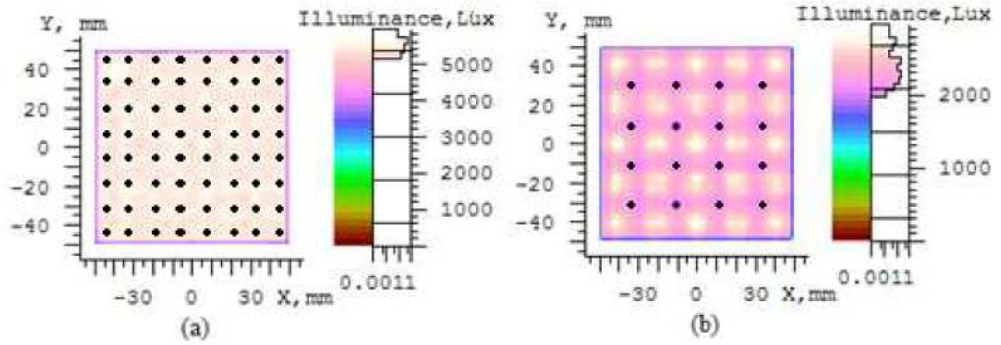

Fig. 16. Simulated illuminance distributions corresponding to peak points (a) d_{p1} = 13.41mm, CV(RMSE) = 0.028 (b) d_{p2} = 20.66mm, CV(RMSE) = 0.087. Black dots are used to state positions of LEDs.

For a LAL system based on LUXEON® Batwing LED with a thickness of 20mm, illuminance distributions corresponding to three zero points have been simulated and designers can select the optimum one among them. The non-monotone-decreasing happens when the separation increase from 13.41mm to 16.66mm.

#128952 - $15.00 USD Received 24 May 2010; revised 26 Jun 2010; accepted 12 Jul 2010; published 30 Jul 2010

Under the same uniformity requirement, the optimum separation of LUXEON® Batwing LED is much smaller than that of LED with freeform lens designed in house, which verifies that larger view angle with lead to smaller package density.

Nowadays, besides the conventional rectangular arrangement, triangular or hexagonal arrangement is also utilized in LAL system due to the advantages such as increased power density [11].

If LEDs with freeform lens designed in house are used to construct an array with triangular arrangement, the analysis is similar. Firstly, the model for calculation is constructed, as shown in Fig. 17. The illuminance in the gray region in Fig. 17 is considered to be generated by 15 neighboring LEDs that make up 16 triangular meshes when the separation between LEDs is large enough. The expression of the illuminance on point (x,y) is derived, as given by Eq. (12). Then by differentiating E(x,y) twice and setting x = 0, y = 0 and z = 20mm, function $f(d)$ is acquired. The functional image of $f(d)$ is shown in Fig. 18.

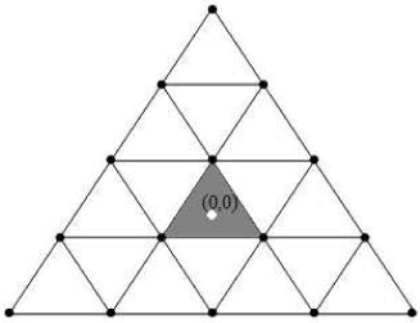

Fig. 17. Model of a LAL system with a triangular array formed up by 15 LEDs. The gray region is a repeated mesh in the system. Black dots states the positions of LEDs. A white dot indicates the origin

$$E(x,y)=\sum_{i=1}^{15} E[\sqrt{(x-x_i)^2+(y-y_i)^2+z^2},\arctan(\frac{\sqrt{(x-x_i)^2+(y-y_i)^2}}{z})] \tag{13}$$

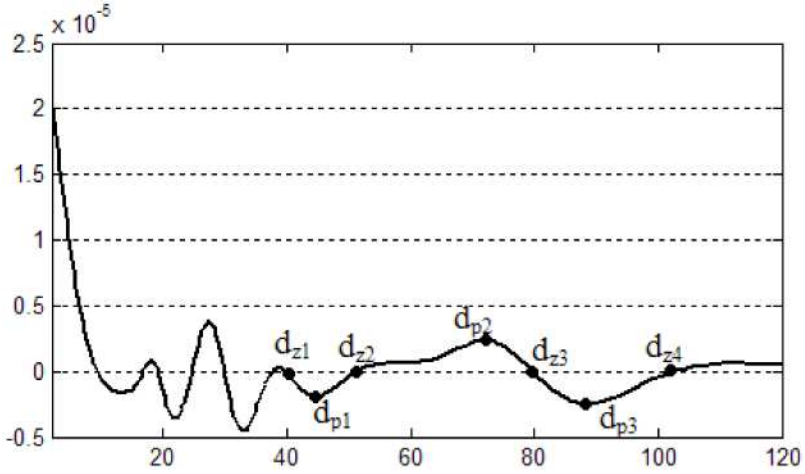

Fig. 18. The functional image of $f(d)=\partial^2 E/\partial x^2 \mid_{x=0,\,y=0,\,z=20}$ in the analysis of triangular arrangement

#128952 - $15.00 USD Received 24 May 2010; revised 26 Jun 2010; accepted 12 Jul 2010; published 30 Jul 2010

Analogously, the zero points, as d_{z1} = 39.80mm, d_{z2} = 51.23mm, d_{z3} = 79.77mm and d_{z4} = 102.60mm are selected for illuminance uniformity analysis by ignoring some smaller zero points. Three peak points, as d_{p1} = 44.72mm, d_{p2} = 72.09mm and d_{p3} = 89.09mm between every two adjacent zero points are also selected to analyze the monotonicity

A triangular array with large number of LEDs and a 300mm × 300mm observation plane were constructed for simulation, The CV(RMSE) value calculated with 900 sampled points corresponding to d_{z1}, d_{z2}, d_{z3} and d_{z4} is 0.067, 0.024, 0.091 and 0.286 respectively while the CV(RMSE) value corresponding to d_{p1}, d_{p2} and d_{p3} is 0.074, 0.130 and 0.303 respectively.

The uniformity increases when the separation increases from 44.72mm to 51.23mm, from 72.09mm to 79.77mm and from 89.09mm to 102.6mm.

A maximal suitable separation should be selected among those zero points and d_{z2} = 51.23mm will be a practicable selection for most applications. Under the same uniformity requirement, the optimum separation for rectangular array is about 65.12mm as discussed before. The optimum separation of triangular array is smaller, which will lead to a higher power density.

The design method for hexagonal arrangement is similar and the procedure will not be repeated in the paper.

While designing a LAL system, we all want to acquire a solution that can meet the requirement of illuminance uniformity with the largest LED-to-LED spacing. For generalized Lambertian LED, some formulas proposed in references [5–8], such as Eq. (6), can be used to calculate the maximal separation directly. However, this method is not practicable for LAL system based on NMDD LED, as simple formulas cannot be acquired to calculate the optimum separation due to the complexity of NMDD. In addition, the uniformity is non-monotone-decreasing with the increasing of separation. The optimum separation may be missed by running simulations with gradually increasing separation due to the nonmonotonicity. Exhausting all the possible separations is unacceptable in time cost.

The derivation in this paper is just to provide references to designers puzzled by this question. LAL system based on large view angle LED exhibits quite different properties from that based on generalized Lambertian LED, such as that there are multiple zero points of the second derivative of the illuminance distribution function. Referring to the method proposed in this paper, it is convenient and time-saving for designers to select the optimum array configuration among those zero points by combining the specific demands of applications. And the non-monotone-decreasing must be noted. A Flow chart is drawn in Fig. 19 to clarify the design method.

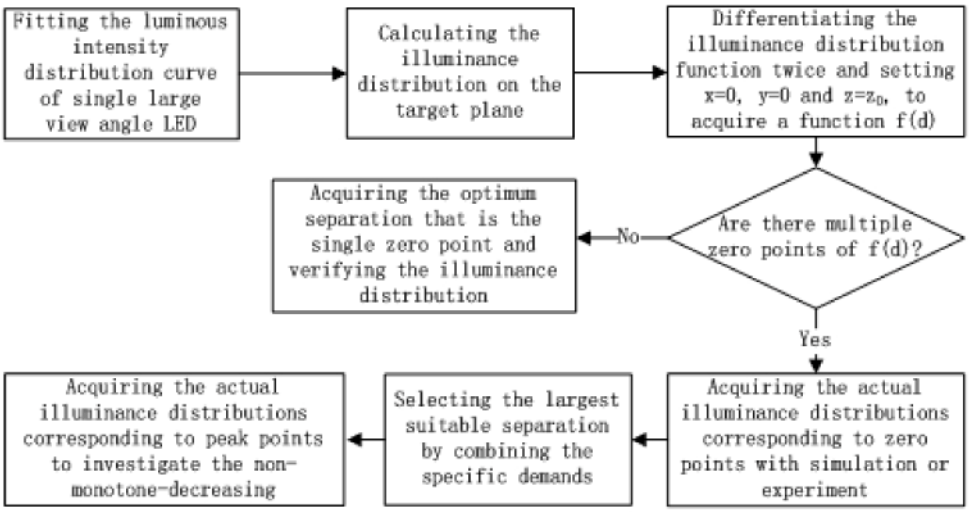

Fig. 19. Flow chart to clarify the method of designing a uniform LAL system with large view angle LEDs

#128952 - $15.00 USD Received 24 May 2010; revised 26 Jun 2010; accepted 12 Jul 2010; published 30 Jul 2010

5. Conclusion

A uniform lighting plane can be acquired by a LED array where the illuminance uniformity is decided by configuration of the LED array and the distance from the array to the target plane. For generalized Lambertian LED, the relationship between the array configuration and height of the target plane has been disclosed expressly and a simple criterion formula has been presented. However, the situation is different for LAL system based on NMDD LED. This paper proposed a method for analyzing the condition for uniform lighting generated by this type of LED. The luminous intensity distribution of a LED with freeform lens that can produce a circular pattern on the target plane was fitted. An LED array with rectangular arrangement was constructed by this type of LED and the condition for uniform lighting was derived on the basis of Sparrow's Criterion. It is found that there are multiple zero points of the second derivative of the illuminance distribution function, which helps the designers selecting the optimum separation combining the specific demands of applications. Moreover, the illuminance uniformity is not monotone decreasing with the increasing of the separation between LEDs. Other type of large view angle LED and different arrangements of LED array was investigated too. As compared with the simulated results and the calculated theory, the method of designing a LAL system based on NMDD LEDs is correct.

Acknowledgements

This work was supported by NSFC Key Project under grant number 50835005, NSFC Project under grant number 50876038, High Tech Project of Ministry of Science and Technology under grant number 2009AA03A1A3 and GuangDong Real Faith Optoelectronics Inc.

#128952 - $15.00 USD Received 24 May 2010; revised 26 Jun 2010; accepted 12 Jul 2010; published 30 Jul 2010